Neural Wiskott-Aldrich syndrome protein modulates Wnt signaling and is required for hair follicle cycling in mice

Anna Lyubimova,[1,2] John J. Garber,[1,2] Geeta Upadhyay,[1,2] Andrey Sharov,[3] Florentina Anastasoaie,[1] Vijay Yajnik,[1,2] George Cotsarelis,[4] Gian Paolo Dotto,[5,6,7] Vladimir Botchkarev,[3,8] and Scott B. Snapper[1,2]

[1]Gastrointestinal Unit and the Center for Inflammatory Bowel Disease, Massachusetts General Hospital, Boston, Massachusetts, USA. [2]Department of Medicine, Harvard Medical School, Boston, Massachusetts, USA. [3]Department of Dermatology, Boston University Medical Center, Boston, Massachusetts, USA. [4]Department of Dermatology, Kligman Laboratories, University of Pennsylvania School of Medicine, Philadelphia, Pennsylvania, USA. [5]Cutaneous Biology Research Center, Massachusetts General Hospital, Boston, Massachusetts, USA. [6]Department of Dermatology, Harvard Medical School, Boston, Massachusetts, USA. [7]Institute of Biochemistry, University of Lausanne, Epalinges, Switzerland. [8]Cutaneous Biology Group, University of Bradford, West Yorkshire, United Kingdom.

The Rho family GTPases Cdc42 and Rac1 are critical regulators of the actin cytoskeleton and are essential for skin and hair function. Wiskott-Aldrich syndrome family proteins act downstream of these GTPases, controlling actin assembly and cytoskeletal reorganization, but their role in epithelial cells has not been characterized in vivo. Here, we used a conditional knockout approach to assess the role of neural Wiskott-Aldrich syndrome protein (N-WASP), the ubiquitously expressed Wiskott-Aldrich syndrome–like (WASL) protein, in mouse skin. We found that N-WASP deficiency in mouse skin led to severe alopecia, epidermal hyperproliferation, and ulceration, without obvious effects on epidermal differentiation and wound healing. Further analysis revealed that the observed alopecia was likely the result of a progressive and ultimately nearly complete block in hair follicle (HF) cycling by 5 months of age. N-WASP deficiency also led to abnormal proliferation of skin progenitor cells, resulting in their depletion over time. Furthermore, N-WASP deficiency in vitro and in vivo correlated with decreased GSK-3β phosphorylation, decreased nuclear localization of β-catenin in follicular keratinocytes, and decreased Wnt-dependent transcription. Our results indicate a critical role for N-WASP in skin function and HF cycling and identify a link between N-WASP and Wnt signaling. We therefore propose that N-WASP acts as a positive regulator of β-catenin–dependent transcription, modulating differentiation of HF progenitor cells.

Introduction

Mammalian skin is composed of 2 structural layers, known as the epidermis and dermis, which are separated by a basement membrane. The epidermis consists of several interconnecting layers of keratinocytes that extend from the basement membrane to the skin surface. During differentiation, basal keratinocytes lose contact with the basement membrane and migrate to suprabasal layers. These cellular movements require changes in cell-cell and cell-matrix adhesion and massive actin cytoskeletal reorganization. Several additional critical physiological processes in skin, such as wound healing and hair follicle (HF) cycling (1–3), also require reorganization of the actin cytoskeleton. Aberrant cytoskeletal regulation is associated with a variety of human disorders of the skin (4, 5).

The Rho family GTPases Cdc42 and Rac1 are critical regulators of the actin cytoskeleton and are essential for skin and hair function (6–8). Cdc42 and Rac are known to control actin dynamics at the leading edge of migrating cells and at adhesive contacts located at cell-cell junctions (i.e., adherens junctions [AJs]). In particular, Cdc42 can induce fingerlike protrusions known as filopodia, and Rac1 promotes the formation of broad leaflike protrusions known as lamellipodia (9–13). Formation of AJs is required for skin integrity and depends on extension of filopodia driven by de novo actin polymerization (14).

Recently, Cdc42 was implicated in regulating skin differentiation through modulation of the Wnt signaling pathway (8). Wnts are secreted glycoproteins that, upon binding and activation of Frizzled receptors, lead to a cascade of signaling events that result in the stabilization and cytoplasmic accumulation of β-catenin. Cytoplasmic β-catenin translocates into the nucleus, where it acts as a co-factor for transcription factors of the Lef1/Tcf family (15, 16). While the majority of cellular β-catenin (>90%) is bound to α-catenin and E-cadherin at AJs (a pool regulated independently of Wnt signaling), a small portion of cytoplasmic β-catenin, which is tightly regulated by Wnt ligands, is constitutively targeted for proteasomal degradation by a complex of proteins (APC, GSK-3β, and axin, termed "destruction complex") in the absence of Wnt stimulation. Upon β-catenin degradation, Lef1/Tcf-mediated gene transcription is impeded (17). Impaired regulation of Wnt signaling can result in an imbalance between proliferation and differentiation and often leads to neoplastic transformation (15, 16, 18).

In skin, Wnt/β-catenin signaling plays a critical role in HF development, hair stem cell maintenance, and HF lineage commitment (19). Transgenic mice expressing constitutively active β-catenin develop extra HFs de novo (20), while deletion of β-catenin (21) or Lef1 (22) or overexpression of the Wnt inhibitor Dkk1 (23) in mice leads to alopecia. De novo HF formation in normal adult mice after wounding was recently described and shown to also depend on Wnt signaling (24). Genes encoding hair keratins are Wnt-dependent transcription targets, as they possess Lef1/Tcf

Conflict of interest: The authors have declared that no conflict of interest exists.
Citation for this article: *J Clin Invest.* 2010;120(2):446–456. doi:10.1172/JCI36478.

binding sequences (25). In postnatal HFs, the strongest Wnt signal has been found in terminally differentiated cortical cells of the hair shaft (26). Wnt signaling in the bulge, a HF stem cell resident niche, is predominantly suppressed, except for a few cells at the beginning of the hair cycle (26, 27). This supports the current theory that Wnt signaling is important for HF stem cell activation and HF cycle initiation.

A connection between Cdc42 and the Wnt signaling pathway was first described in cultured astrocytes (28). Cdc42 modulates β-catenin turnover by regulating GSK-3β phosphorylation of a critical serine residue through the Par6/Par3/PKCζ complex. Recently, it has been shown in skin that Cdc42 controls GSK-3β phosphorylation via modulating PKCζ activity, and the absence of Cdc42 leads to a decrease in GSK-3β phosphorylation (8). This reduction results in increased GSK-3β kinase activity, leading to an increased phosphorylation of axin and β-catenin. Finally, this leads to stabilization of the destruction complex, degradation of β-catenin, and a decrease in β-catenin–dependent transcription of HF-specific genes (8).

Here we examine the role of neural Wiskott-Aldrich syndrome protein (N-WASP), the ubiquitously expressed Wiskott-Aldrich syndrome–like (WASL) protein and direct target of Cdc42, in skin function. Activated by Cdc42, N-WASP is a critical regulator of the actin cytoskeleton through its modulation of Arp2/3 complex–mediated actin assembly. While WASL proteins regulate diverse processes such as cell movement, adhesion, and phagocytosis (29, 30), no studies have examined the role of WASL family proteins in epithelial function in vivo. In this report, we demonstrate that conditional N-WASP deletion in skin results in marked epidermal hyperproliferation, ulceration, and alopecia, while terminal keratinocyte differentiation and wound healing are unaffected. We demonstrate that alopecia results from a progressive and finally severe HF cycle defect. Interestingly, although in young N-WASP epidermal KO (EKO) mice there is an increase in the number of follicles entering the anagen phase compared with WT mice that is associated with increased proliferation in the stem cell compartment, there is a nearly complete block in HF cycling in 5-month-old animals. Moreover, N-WASP deficiency was accompanied by a dramatic decrease in GSK-3β phosphorylation, leading to decreased nuclear localization of β-catenin and decreased Wnt-dependent transcription, which may ultimately contribute to the age-dependent stem cell depletion in the HF. Our study shows a critical role for N-WASP in skin function and HF cycling and provides a link between N-WASP and Wnt signaling. We propose that N-WASP acts as a positive regulator of β-catenin–dependent transcription to regulate HF progenitor cell differentiation.

Results

Generation of mice with N-WASP deletion in skin. Germline deletion of *N-Wasp* results in early embryonic lethality (31, 32). In order to study the role of N-WASP in adult tissues, we generated mice in which exon 2 of *N-Wasp* was flanked by loxP sites (*N-Wasp*^{L2L}), permitting its conditional deletion (33). Since *N-Wasp*$^{L2L/L2L}$ mice were indistinguishable from WT animals, these animals are referred to throughout the text as WT. To eliminate N-WASP in the epidermis, we crossed *N-Wasp*$^{L2L/L2L}$ mice with CrePR1 transgenic mice under the control of the keratin 5 promoter, which is active in epidermal keratinocytes and other squamous epithelia (Figure 1) (34). Tissue-specific Cre activation has been reported to require treatment with the antiprogestin RU486 to induce translocation of the enzyme to the nucleus, where it catalyses DNA recombination (35). However, spontaneous CrePR1 recombinase activation has been reported in mice during the first postnatal weeks depending on the quantity of expressed protein (36). We found spontaneous tissue-specific Cre activation in the absence of inducer with excision of exon 2 of *N-Wasp* in the epidermis of *N-Wasp*$^{L2L/L2L}$*; K5-CrePR1* mice (i.e., N-WASP EKO mice; Figure 1). Spontaneous exon 2 excision was also detected in thymus, esophagus, foregut, and tongue, tissues in which the K5 promoter is known to be active (Figure 1A). In tissues in which the K5 promoter is inactive, such as colon and skeletal muscle, the excision was not detected (Figure 1A). Western blot analysis of protein lysates derived from the epidermis in the absence of RU486 showed incomplete *N-Wasp* excision at postnatal day 15 with complete excision between postnatal days 15 and 25 (Figure 1B, lanes 1–4). N-WASP was also completely ablated in primary cultured keratinocytes, derived from untreated 3-day-old N-WASP EKO mice (Figure 1B, lanes 5 and 6). We did not use RU486 induction in our further experiments, since the efficiency and timing of spontaneous N-WASP ablation was highly reproducible.

N-WASP is critical for keratinocyte proliferation and hair growth. By 4–5 weeks of age, N-WASP EKO animals had subtle thinning of hair with the development, in some animals, of facial ulcers (Figure 2A). Hair loss was progressive, with all animals displaying thinning of the hair coat by 12 weeks of age (Figure 2A). By 20 weeks of age, all N-WASP EKO mice were nearly bald with multiple ulcerations without evidence of an ongoing inflammatory process (Figure 2A and data not shown). N-WASP EKO mice progressively failed to gain weight (12 weeks: WT, 30.4 ± 1.7 g, N-WASP EKO, 24.9 ± 4.7 g, $P < 0.05$, $n = 4$; 15 weeks: WT, 38.2 ± 2.9 g, EKO, 24.8 ± 4.5 g, $P < 0.05$, $n = 9$; 17 weeks: WT, 35.5 ± 3.8 g, EKO, 21.0 ± 3.6 g, $P < 0.01$, $n = 3$), and most were unable to breed by the 16th week and required euthanasia.

Histological analysis of skin taken from ulcer-free areas of N-WASP EKO mice showed a significant increase in epidermal thickness (Figure 2D). As expected, these changes were associated with a dramatic increase in Ki-67 immunoreactive nuclei in the basal layer of EKO epidermis (Figure 2D). Consistent with these findings, in vivo BrdU incorporation assays revealed a marked increase in proliferation in primary keratinocytes freshly isolated from EKO mice ($P = 0.005$; Figure 2B). Similarly, cultured primary keratinocytes also demonstrated significantly increased proliferation by BrdU incorporation assays (Figure 2C). These findings indicate that hyperproliferation is an intrinsic characteristic of the N-WASP–deficient keratinocytes and not a consequence of ongoing hair loss and/or an inflammatory process.

N-WASP is not required for epidermal differentiation or wound healing. Defects in proliferation in skin can be associated with defects in keratinocyte differentiation (37). Given the proliferative abnormalities in N-WASP EKO mice and the dependence of keratinocyte differentiation upon reorganization of the actin cytoskeleton (13, 37), a process known in other systems to be regulated by N-WASP (29), we investigated keratinocyte differentiation. Despite altered cell proliferation, there were no obvious abnormalities in the distribution of early (keratin 1) or late (loricrin, filaggrin) differentiation markers in N-WASP EKO epidermis (Figure 2E).

Keratinocyte differentiation can be modeled, at least in part, in culture (38). Primary keratinocytes maintained in a low-calcium–containing medium (0.05 mM) express characteristics of the nondifferentiated basal cell compartment, whereas culturing in a higher-calcium–containing medium (2.0 mM) induced differentiation associated with growth arrest, AJ formation, loss of cell substrate

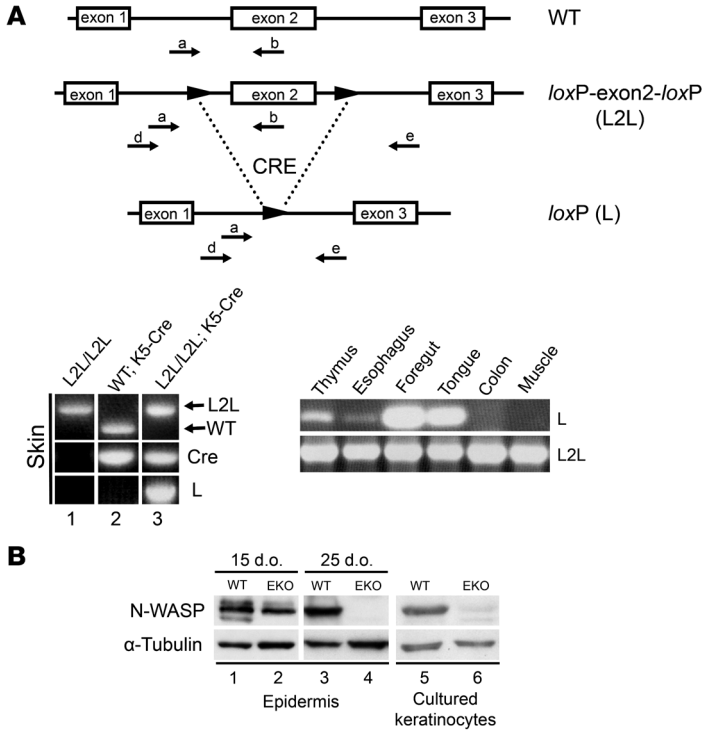

Figure 1
Epidermis-specific KO of N-WASP. (**A**) Top: PCR strategy to detect exon 2 deletion of *N-Wasp*. Primers used to determine presence (a, b) or absence (d, e) of exon 2. Bottom left: PCR amplification of tail DNA from 4-month-old *N-Wasp*$^{L2L/L2L}$ (L2L/L2L) mice with and without the *K5-Cre* transgene and a WT mouse with the *K5-Cre* transgene. Amplification of WT and L2L/L2L DNA with primers a and b resulted in a 350-bp band (lane 2 WT) and a 550-bp band (lane 1 L2L), respectively. Amplification of WT DNA with primers d and e failed to yield a product (lane 2 L). Amplification with primers d and e resulted in a 1.5-kb band, thus identifying the excision of exon 2 in *L2L/L2L; K5-Cre* mice (lane 3 L). The presence or absence of Cre is noted by separate PCR amplification in the middle row. Bottom right: Gel electrophoresis of DNA from different tissues of a 4-month-old *N-Wasp*$^{L2L/L2L}$*/K5-Cre* mouse following PCR with primer sets to determine the presence (L2L, primers a and b) or absence (L, primers d and e) of exon 2. Exon 2 excision was observed in thymus, esophagus, foregut, and tongue. (**B**) Western blot analysis of N-WASP expression in epidermis (lanes 1–4) and cultured keratinocytes (lanes 5 and 6) isolated from L2L (referred to as WT) and *N-Wasp*$^{L2L/L2L}$*/K5-Cre* (*L2L; K5-Cre* – i.e., EKO) mice. Epidermis was isolated from 15- and 25-day-old mice, and primary keratinocytes were isolated from 3-day-old mice and maintained in culture for 5 days. N-WASP expression was undetectable in EKO mice.

contact, and expression of early and then late markers of differentiation (39). Using Western blot analysis, we found that the expression of neither early (keratin 1) nor late (loricrin, involucrin, or filaggrin) differentiation markers was altered in the absence of N-WASP in calcium-treated cultured primary keratinocytes (data not shown). Taken together, these data indicate that epidermal keratinocytes can terminally differentiate in the absence of N-WASP.

Epithelial wound closure is known to depend on cell migration. Since cell migration critically depends on actin cytoskeleton integrity and dynamics, and WASP family members are known to control actin polymerization, we hypothesized that skin ulcerations in N-WASP EKO animals may result from a wound-healing defect. We tested the role of N-WASP in epidermal wound healing by comparing wound re-epithelialization in WT and N-WASP EKO mice. Wounds 6 millimeters in diameter (full thickness) were incised on the back skin of WT and N-WASP EKO mice, and wound closure was assessed by immunohistochemical analysis of H&E-stained sections at various times after injury. Quantitative analyses of wound re-epithelialization (by measuring the length of neo-epithelium; dashed line in Supplemental Figure 1; supplemental material available online with this article; doi:10.1172/JCI36478DS1) in WT and N-WASP EKO mice revealed similar rates of wound healing (Supplemental Figure 1). These results indicate that wound healing can proceed normally in the absence of N-WASP. N-WASP–deficient skin showed no signs of increased inflammation or abnormal vascularity, suggesting that aberrant immune activity or microvascular architecture was not responsible for the epidermal ulceration.

N-WASP is essential for HF cycling. Since N-WASP EKO mice develop progressive alopecia, we sought to determine whether there were any alterations in HF maturation in unmanipulated N-WASP EKO skin. The first postnatal HF cycle in N-WASP EKO mice was not affected (data not shown). This was expected, since N-WASP ablation in skin was not complete until postnatal day 25. Although there were subtle differences in the thickness of the hair coat at 30 days of age, we found no significant differences in the number of anagen follicles in N-WASP EKO mice compared with WT mice at this age (Figure 3B). However, in 8-week-old mice, surprisingly most (75%) N-WASP EKO HFs were in early anagen phase, at a time when the majority of follicles (75%) in WT mice were in telogen phase (Figure 3, A and B). By 10 weeks of age, nearly all HFs in EKO mice were in either telogen phase (48.6%) or late catagen phase (49.7%), with very few anagen-phase follicles persisting. This was in contrast to 10-week-old WT mice, which exhibited approximately 30% of HFs in anagen; the remainder of follicles were in telogen phase (67%), with less than 5% in catagen phase (Figure 3B). The rapid decline of anagen-phase follicles that occurred between 8 and 10 weeks of age may suggest that the increased number of anagen-phase HFs observed in 8-week-old EKO mice represents precocious entry into anagen phase, rather than an increased duration of the first postnatal anagen phase.

Given the aberrant follicular stage in young mice and progressive alopecia, we sought to determine whether HF cycle progression was normal in synchronized N-WASP EKO skin. HF regeneration — the hallmark of the anagen phase — can be synchronized by hair plucking (depilation) during telogen phase (40). With depilation, the growth stage (anagen) is induced and keratinocytes next to the dermal papilla start to proliferate. Three days after depilation, the proliferating keratinocytes partially surround an enlarged dermal papilla (anagen II). As the anagen phase progresses the growing follicle increases its length (with the hair bulb now residing in the subcutis), inner root sheaths and outer root sheaths (ORSs) form, and actively proliferating matrix keratinocytes completely surround a narrowed dermal papilla (anagen III). By anagen IV, matrix cells have differentiated, forming a precortex and a hair shaft (Figure 4A).

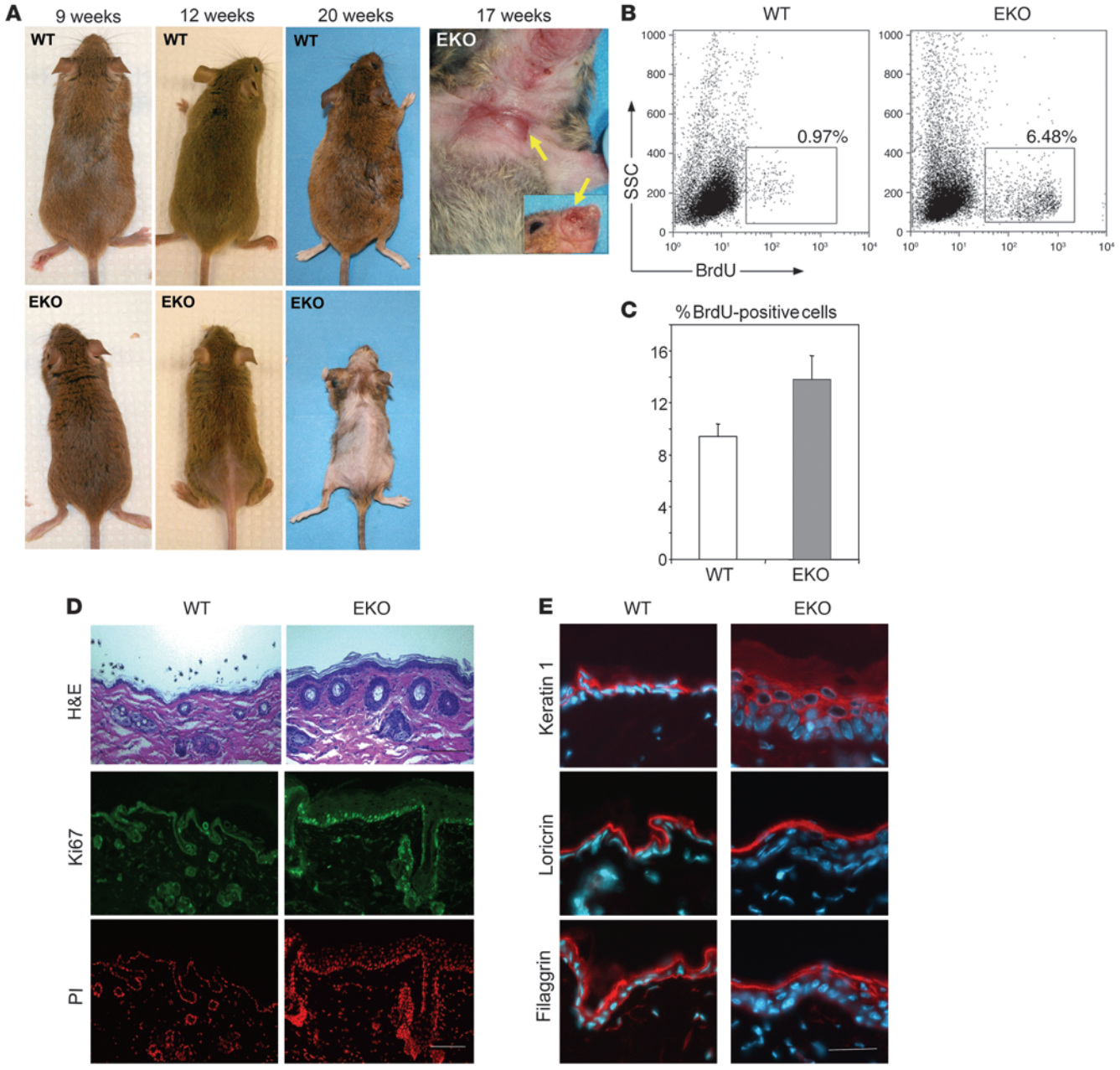

Figure 2

Hair loss, ulceration, and epidermal hyperproliferation in N-WASP EKO mice. (**A**) WT and EKO littermate mice 9, 12, and 20 weeks old. Ulcers (arrows) on the chest and face of a 17-week-old EKO mouse are also shown. (**B**) Representative FACS analysis of primary keratinocytes. Keratinocytes were isolated from mice 2 hours after BrdU injection and analyzed by flow cytometry. Selected (gated) events represent the total percentage of $BrdU^+$ keratinocytes in the representative experiment; average $BrdU^+$ in EKO mice was 5.1% (n = 11) vs. WT 1.0% (n = 10) (P = 0.004). (**C**) Results of proliferation analysis of primary keratinocytes in culture. Cultured keratinocytes were labeled with BrdU for 30 minutes, fixed, stained with anti-BrdU antibody, and analyzed by flow cytometry. The results of 1 representative experiment (repeated 3 times) are shown; each bar represents mean value of 6 samples ± SD. (**D**) H&E-stained paraffin skin sections of WT and EKO mice demonstrate an expansion/hyperproliferation of HFs and interfollicular epidermis (upper panel, arrows). Frozen skin sections were stained with the antibody against the proliferation marker Ki-67 (green), and nuclei were stained with propidium iodide (PI, red). The increased epidermal proliferation was associated with an increase in $Ki\text{-}67^+$ nuclei. Scale bar: 100 mm. (**E**) Normal distribution of early (keratin 1) and late (loricrin, filaggrin) markers of differentiation in hyperproliferative N-WASP–deficient epidermis. Frozen sections stained with antibodies against keratin 1, loricrin, and filaggrin (red). Nuclei were counterstained with Hoechst (blue). Scale bar: 40 mm.

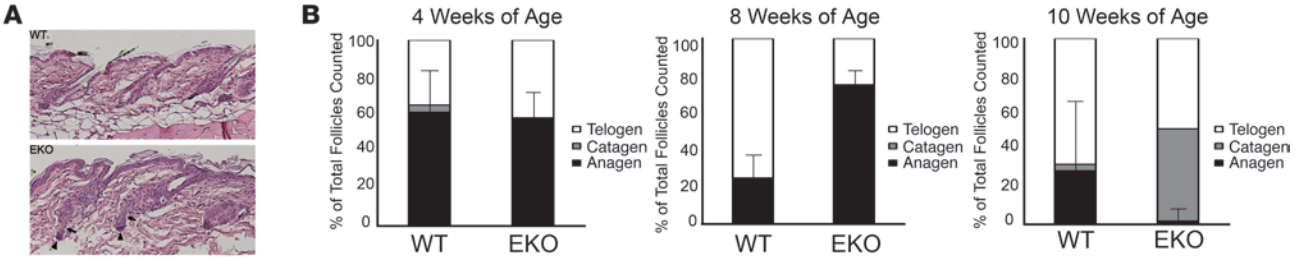

Figure 3
N-WASP EKO mice exhibit an increased number of anagen-phase HFs compared with WT mice at 8 weeks of age, which rapidly declines by 10 weeks. (**A**) H&E staining of the WT and N-WASP EKO skin. WT follicles were predominantly in telogen phase. The majority of N-WASP EKO follicles showed typical characteristics of beginning anagen phase, such as proliferation-driven thickening and elongation of keratinocyte strand (arrows) near dermal papilla (arrowheads). Original magnification, ×20. (**B**) Analysis of HF changes over time in unmanipulated WT and N-WASP EKO mice at 4 weeks (n = 8), 8 weeks (n = 10), and 10 weeks (n = 6) of age. HFs in anagen, telogen, and catagen phases were scored and expressed as a percentage of the total number of follicles counted. Error bars indicate the SD of anagen-phase follicles.

We first compared HF cycle progression in 18- to 20-week-old WT and N-WASP EKO mice (at this age, all mice had severe but not complete alopecia). HFs were synchronized by wax depilation of patches where hair was present on sex-matched WT and N-WASP EKO mice, and skin sections were analyzed histologically. Keratinocyte proliferation was assessed concurrently by BrdU incorporation. All WT HFs reach anagen IV within 6 days after depilation (Figure 4, A–C, arrows point to proliferating matrix cells). In contrast, virtually all follicles examined in N-WASP EKO mice 6 days after hair depilation remained in telogen (Figure 4, D and E), with only 1 N-WASP EKO mouse examined (n = 11) containing any anagen follicles. Whereas follicles in WT mice have progressed to anagen IV (Figure 4, B and C), no follicles in the single N-WASP EKO mouse progressed past anagen II (data not shown). HF keratinocytes in all of the other 18- to 20-week-old N-WASP EKO animals examined 6 days after depilation failed to proliferate (Figure 4E, arrows), consistent with telogen phase.

We next sought to characterize the effects of N-WASP deletion on earlier HF cycles in younger mice (at ages in which the alopecia is mild). HFs in 8- to 13-week-old mice were induced by depilation and analyzed as above. As expected, HFs entered anagen phase appropriately in all WT animals examined (Figure 4F and Supplemental Figure 2A), with matrix keratinocyte proliferation, consistent with anagen II and IV (Supplemental Figure 2B and Figure 4G, respectively). In 28% of N-WASP EKO animals examined at this age (n = 18), HFs failed to enter anagen phase and remained in telogen phase (Figure 4H and Supplemental Figure 2C), with no evidence of BrdU incorporation in HFs (Figure 4I and Supplemental Figure 2D, arrows). In the remaining 72% of N-WASP EKO animals at 8 to 13 weeks of age, HFs entered anagen phase and progressed to anagen II (Supplemental Figure 2, E and F) and anagen IV (Figure 4, J and K). However, most anagen HFs in N-WASP EKO mice appeared abnormal with severe hyperplasia of the upper follicle and interfollicular epidermis (Figure 4, J and K, and Supplemental Figure 2F, open arrowheads). These results indicate a progressive and eventually severe impairment of HF cycling after N-WASP excision in epidermis.

N-WASP is critical for the maintenance and proper differentiation of HF progenitor cells. HF cycling requires the continuous supply of skin progenitor cells that reside in a specialized microenvironment of the hair appendage called the bulge. These progenitor cells can be distinguished by the expression of 2 well-characterized skin stem cell markers, CD34 and α6 integrin (41). This population of skin stem cells can be further subdivided into a $CD34^+/\alpha6^{hi}$ and $CD34^+/\alpha6^{lo}$ population, which correspond to their basal and suprabasal bulge locations, respectively. $CD34^+/\alpha6^{lo}$ stem cells emerge as a distinct subpopulation after the first postnatal anagen phase as a result of the involution of the club hair and establishment of the permanent HF bulge, and remain stable over time (41). Given the altered HF dynamics and progressive alopecia in N-WASP EKO skin, we examined these progenitor populations over time. At 8 weeks of age, N-WASP EKO mice had an increase in the total $CD34^+/\alpha6^+$ stem cell population, but by 16 weeks of age the relative proportion of this population appeared diminished and by 28 weeks of age was dramatically decreased compared with WT (Figure 5A). While the proportion of the distinct $CD34^+/\alpha6^{hi}$ and $CD34^+/\alpha6^{lo}$ keratinocyte populations within the total $CD34^+/\alpha6^+$ stem cell population was comparable or increased at 8 weeks, we also observed a progressive decrease in these important, highly self-renewing and multipotent subpopulations at 16 and 28 weeks in EKO mice (Figure 5A). Notably, EKO mice exhibited this decrease in $CD34^+/\alpha6^+$ progenitor cells despite dramatically increased proliferation within this population as assessed by BrdU incorporation (Figure 5B, EKO average 2.1% vs. WT 0.21% at 16 weeks old; $P < 0.01$). The increase in BrdU incorporation by $CD34^+/\alpha6^+$ stem cells in EKO mice was observed at early time points (8 weeks of age), when this population was comparable to or increased compared with WT, suggesting that abnormal proliferation precedes the decrease in stem cells and is not a response to the ongoing depletion of this population. Together, these results suggest a depletion of skin stem cells over time, which may be a consequence of abnormal proliferation leading to exhaustion of the stem cell compartment.

The ORS is a layer of cells existing in continuity with the bulge and represents the direct path for stem cells migrating from the bulge to the base of the HF during anagen (42). The ORS can be identified by flow cytometry as a transient $CD34^{lo/-}/\alpha6^{lo}$ population appearing in early anagen phase (43, 44). We observed an expanded and persistent population of $CD34^{lo/-}/\alpha6^{lo}$ ORS keratinocytes in EKO mice (Figure 5A). This pattern may result from the continual transit of proliferating bulge stem cells to the ORS.

N-WASP regulates GSK-3β phosphorylation and Wnt-dependent transcription. HF development and cycling critically depends on stabi-

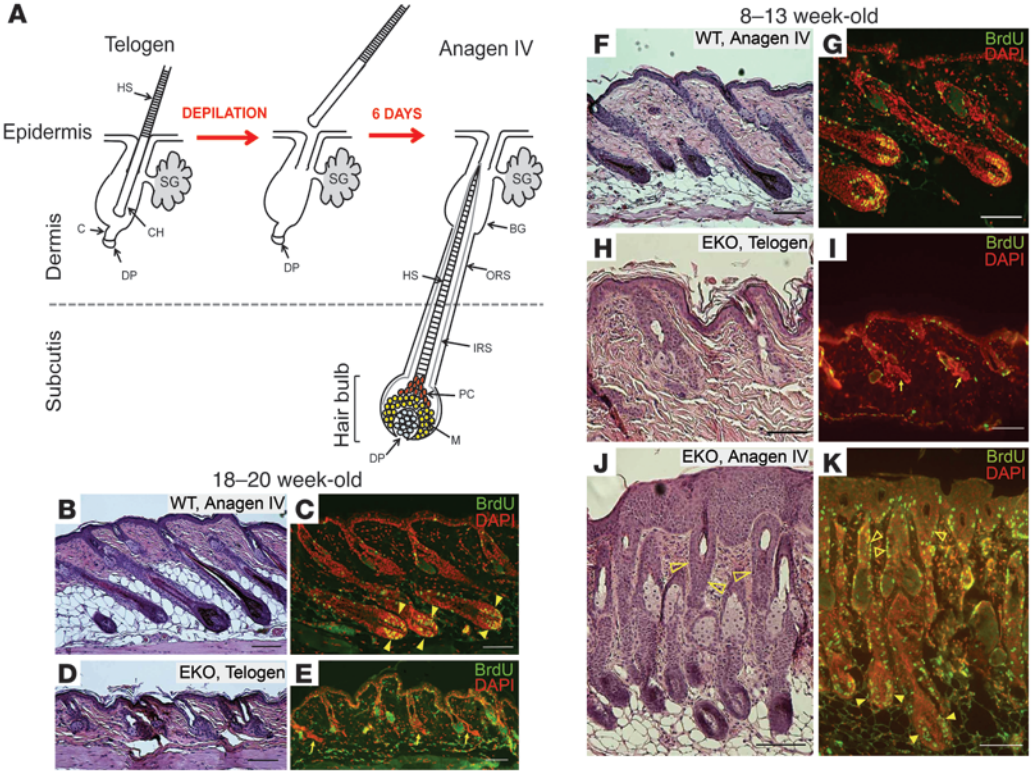

Figure 4

Progressive HF cycling defect in the absence of N-WASP. (**A**) Schematic showing progression of WT HF from telogen to anagen IV phase 6 days after hair depilation. BG, bulge; C, germ cell cap; CH, club hair; DP, dermal papilla; HS, hair shaft; IRS, inner root sheath; M, matrix; PC, precortex; SG, sebaceous gland. (**B**–**E**) HF cycle block in 18-week-old N-WASP EKO mice. HFs were induced by wax depilation in WT (**B** and **C**) and N-WASP EKO (**D** and **E**) female mice and tissue collected on the sixth day after depilation to observe follicles in anagen IV. (**F**–**K**) Partial HF cycle block in 8- to 13-week-old N-WASP EKO mice. Again, skin samples were collected 6 days after depilation from WT (**F** and **G**) and N-WASP EKO (**H**–**K**) female mice to observe follicles in anagen IV. All animals were injected with BrdU prior tissue collection, as described in Methods. Paraffin sections were stained by H&E (**B**, **D**, **F**, **H**, and **J**) or indirectly immunostained with antibodies against BrdU, and all nuclei were counterstained with DAPI (**C**, **E**, **G**, **I**, and **K**). Arrows indicate N-WASP EKO follicles lacking proliferating cells. Filled arrowheads indicate proliferating matrix cells. Open arrowheads indicate hyperproliferation in upper N-WASP EKO follicles. Scale bars: 100 mm.

lization and nuclear localization of β-catenin, followed by LEF-1–mediated transcription (21, 23, 26). Cdc42 modulates β-catenin levels via binding to the target protein Par6, which, in a complex with Par3 and PKCζ, leads to phosphorylation of GSK-3β on serine 9, resulting in β-catenin stabilization (28). Such Cdc42-dependent regulation of β-catenin stability was recently found to control HF progenitor cell differentiation (8). Since N-WASP is a direct target of Cdc42 (29), we investigated the effect of N-WASP deletion on signaling pathways that regulate β-catenin stability and β-catenin–dependent transcription.

To investigate a role for N-WASP in regulating β-catenin–dependent transcription in N-WASP–deficient fibroblast cell lines (32), we used a TopFLASH reporter assay. N-WASP–deficient cells were transformed with a β-catenin–responsive luciferase reporter construct, and the reporter activity was measured following Wnt ligand stimulation. There was a marked decrease in TopFLASH reporter activity in Wnt-stimulated N-WASP–deficient cells when compared with control cells (Figures 6A). In addition, overexpression of N-WASP by stable retroviral transduction led to a modest increase in TopFLASH reporter activity in either WT or N-WASP KO fibroblasts (data not shown). Our data indicate that N-WASP is required for Wnt-dependent transcription.

We next used an immunohistochemical approach to examine β-catenin expression and localization in N-WASP EKO HFs and epidermis. We determined β-catenin localization in skin sections taken from 8- to 13-week-old WT and N-WASP EKO mice and quantified the percentage of HFs with nuclear β-catenin in precortical keratinocytes. In agreement with previously reported data (26), nuclear β-catenin was seen in the subcortex of more than 97% WT anagen HFs (Figure 6, B and C; Supplemental Figure 3A). In N-WASP EKO animals in which HF cycling was completely blocked and all HFs were in telogen (28% of analyzed N-WASP EKO mice at 8 to 13 weeks of age; $n = 18$), nuclear β-catenin was not detected (Supplemental Figure 3A). Since the subcortex is absent in telogen-phase follicles, it remains unclear from these data whether the absence of nuclear β-catenin precedes the hair cycling block or is a consequence of the block and the absence of subcortical keratinocytes. We therefore scored N-WASP–deficient HFs in 8- to 13-week-old mice that progressed through anagen phase for the presence of nuclear β-catenin in subcortical keratinocytes. On average, we found that less than 40% of N-WASP EKO anagen follicles contained nuclear β-catenin (Figure 6, B and C). As predicted, nuclear β-catenin was not detected in the single 18-week-old N-WASP EKO animal described above containing anagen II follicles (Supplemen-

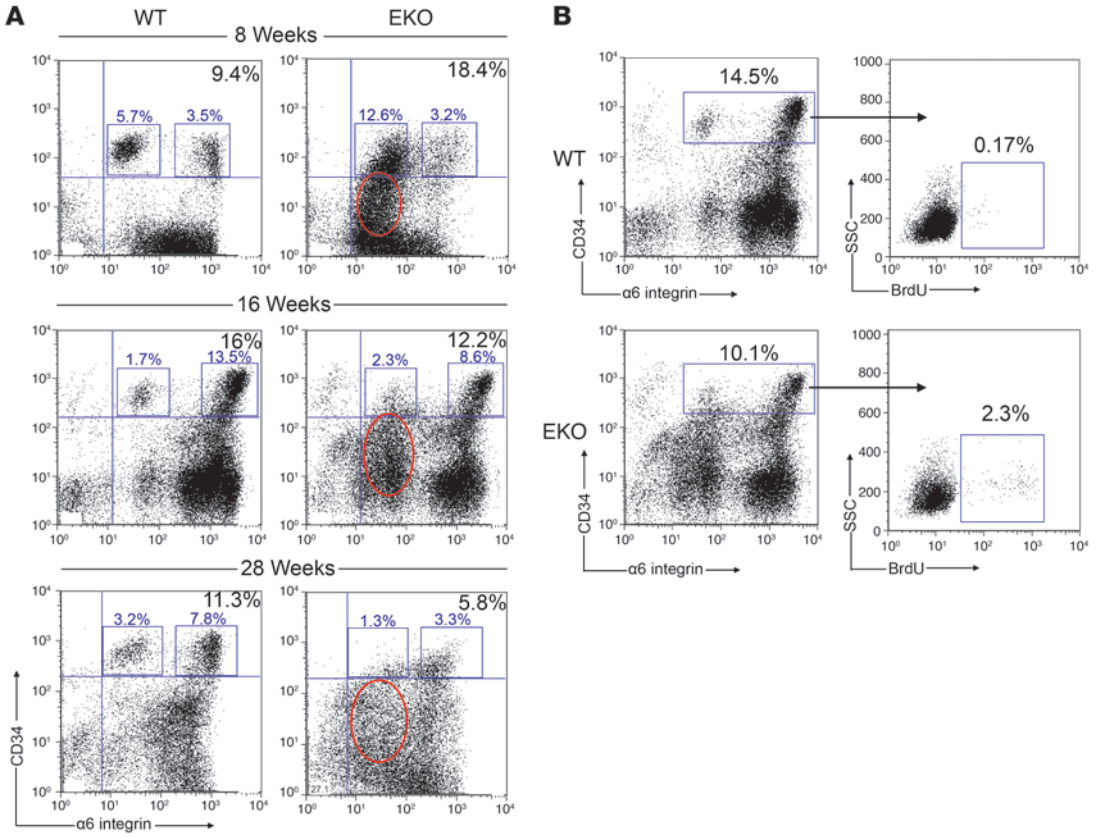

Figure 5

N-WASP EKO mice exhibit a progressive decline in HF stem cells. (**A**) Representative FACS analysis on primary keratinocytes isolated at 8, 16, and 28 weeks of age revealed an initial increase in $CD34^+/\alpha6^+$ progenitor cells in N-WASP EKO mice. This population diminished over time and was dramatically decreased at 28 weeks. Additionally, there was an early appearance and persistence of a $CD34^{lo/-}/\alpha6^{lo}$ population (red circles) corresponding to an abnormal expansion of ORS keratinocytes in N-WASP EKO mice. Selected (gated) events in each plot represent the percentage of $\alpha6^{lo}$ (left boxes) and $\alpha6^{hi}$ (right boxes) cells in the total $CD34^+/\alpha6^+$ population. (**B**) FACS analysis of BrdU incorporation by keratinocytes gated for the stem cell population revealed increased proliferation specifically within this population in N-WASP EKO mice. Gated events in the left panels represent the percentage of $CD34^+/\alpha6^+$ keratinocytes. Gated events in the right panels indicate the percentage of $BrdU^+$ keratinocytes within the selected $CD34^+/\alpha6^+$ population.

tal Figure 3B). As expected, nuclear β-catenin was not detected in telogen-phase follicles from older N-WASP EKO mice (Supplemental Figure 3B). These data suggest that defects in β-catenin localization occur earlier than the HF cycle block.

β-catenin stability is regulated by a complex of several molecules that bind β-catenin and target it for degradation (16). GSK-3β, a member of the complex, phosphorylates axin, which stabilizes the complex and leads to β-catenin degradation. Upon stimulation with Wnt ligand, this event can be prevented by phosphorylation of GSK-3β on serine 9, resulting in its inactivation. To determine the molecular pathway controlling β-catenin stability in N-WASP EKO animals, we assessed GSK-3β phosphorylation on serine 9 in WT and N-WASP–deficient skin by Western blotting. Remarkably, the level of phosphorylated GSK-3β was significantly decreased in N-WASP EKO epidermis from mice 8 weeks of age when compared with WT littermates (Figure 6D). In 18-week-old animals, the reduction of phosphorylated GSK-3β in N-WASP EKO mice was even more pronounced (Figure 6D). These results support the hypothesis that N-WASP is involved in modulating Wnt signaling and β-catenin–dependent transcription. In addition, these results suggest that a defect in Wnt signaling develops gradually over time in skin after N-WASP ablation.

In order to assess the effect of N-WASP ablation on Wnt/β-catenin signaling in vivo, we crossed WT and EKO mice with TopGAL reporter mice, which harbor a β-galactosidase gene under the control of a β-catenin and LEF/TCF-responsive promoter (26). At 8 weeks of age, when EKO mice exhibited mild signs of hair coat thinning and a greater proportion of anagen phase HFs compared with WT mice, EKO/TopGAL mice displayed globally decreased X-gal staining, and, most notably, a near absence of TopGAL activity in the vicinity of the hair germ in late telogen/early anagen HFs (Figure 6E).

Discussion

N-WASP regulates keratinocyte proliferation, but is not required for wound healing or terminal differentiation. This study reveals that N-WASP deficiency leads to epidermal hyperproliferation, indicating that N-WASP negatively regulates keratinocyte growth. To date, molecular mechanisms connecting N-WASP to cell proliferation in keratinocytes are unknown, and current evidence of any link between WASPs and cell growth is scarce. It was recently revealed that an absence or decrease in WASP family protein expression in T cells has been associated with a decrease in cell proliferation (33). In contrast, N-WASP has been implicated as a tumor suppressor in breast epithe-

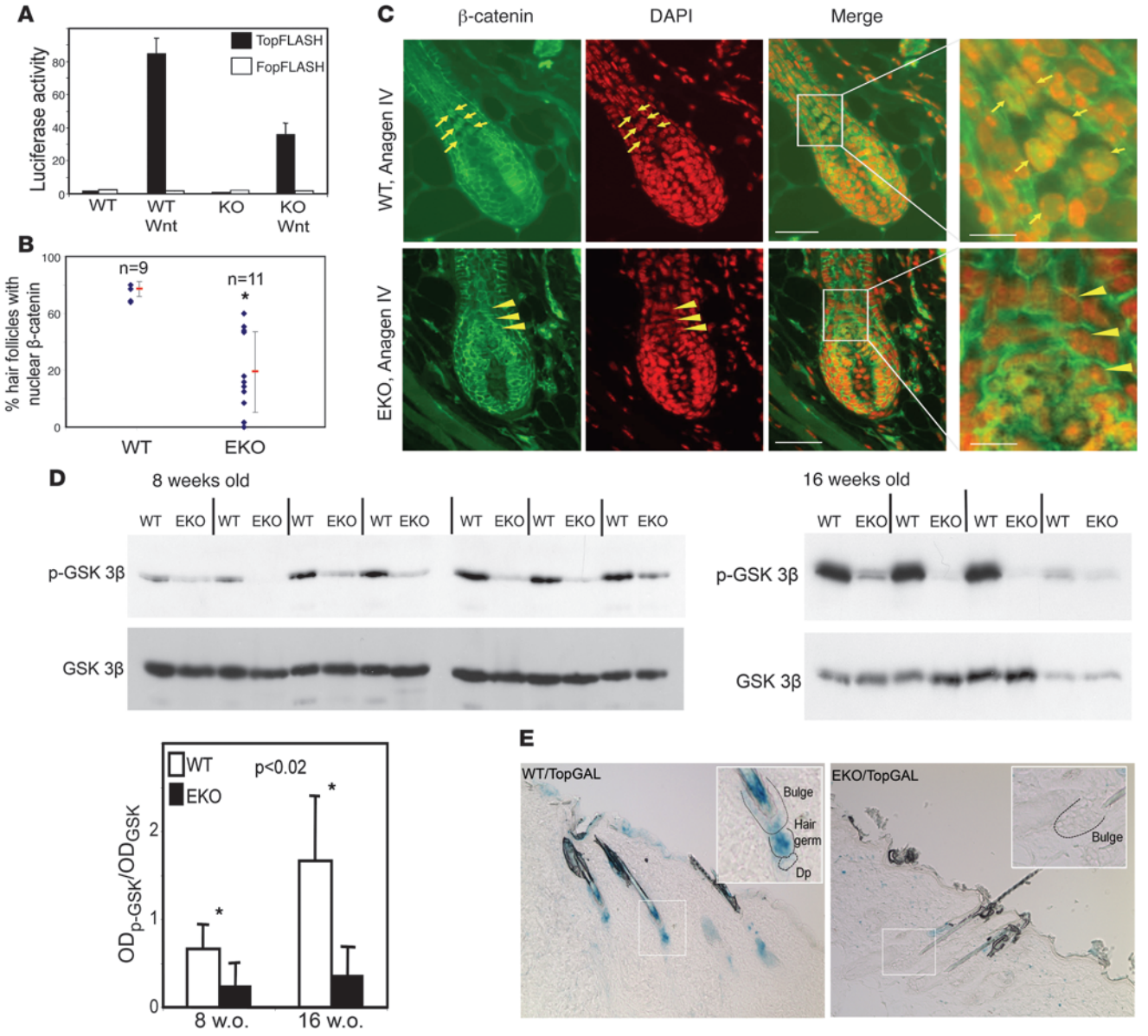

Figure 6

Defective Wnt signaling in N-WASP–deficient epidermis. (**A**) Decrease in Wnt-dependent transcription in N-WASP KO fibroblasts. WT and N-WASP KO fibroblasts or cells expressing a Wnt-responsive (TopFLASH) or a mutant (FopFLASH) reporter construct. Bar graph represents reporter activity upon Wnt stimulation (normalized). Error bars represent SD. Representative results of 1 of 3 experiments are shown. (**B** and **C**) Defect in nuclear localization of β-catenin in N-WASP–deficient HF keratinocytes. Anagen IV follicles in 8-week-old WT (**C**, upper panels) and N-WASP EKO (**C**, lower panels) mice. Green indicates β-catenin antibody staining; red indicates nuclei stained with DAPI; arrows indicate β-catenin–positive nuclei in precortical keratinocytes in WT follicles; arrowheads indicate nuclei devoid of β-catenin in precortical cells of N-WASP–deficient follicles. Scale bar: 40 mm (inset bar, 12 mm). Scatter plot (**B**) represents the percentage of anagen IV follicles with nuclear β-catenin in the subcortex in WT and N-WASP EKO mice. Each dot represents 1 mouse. Vertical lines indicate the mean (middle dash) ± SD. *$P < 0.001$. (**D**) Decrease in serine 9–phospho–GSK-3β in N-WASP EKO skin. Each lane on the Western blot represents 1 mouse. Bar graph depicts the OD of the phospho–GSK-3β band (upper panel) normalized to the OD of the total GSK-3β band (lower panel). Error bars represent SD. (**E**) Decreased Wnt-dependent transcription in N-WASP EKO HFs. Skin from non-depilated 8-week-old WT/TopGAL and EKO/TopGAL mice was processed for X-gal staining. Blue color corresponds to active Wnt-dependent transcription. Original magnification, ×10 (inset, ×20).

lium (45). One can speculate that N-WASP, via its apparent effect on actin cytoskeleton dynamics, regulates keratinocyte adhesion to the extracellular matrix, a process known to control keratinocyte growth (37). In addition, keratinocytes are known to be a source and a target for several cytokines affecting cell proliferation (46). It is possible that, in the absence of N-WASP, the production of cytokines and/or their receptors may be altered. In support of this hypothesis, studies from our laboratory have demonstrated that colonic lamina propria T cells from WASP-deficient animals produce elevated levels of IL-4, a cytokine known to induce keratinocyte proliferation (47).

Surprisingly, we have found that epidermal differentiation and wound healing, processes that are associated with marked cytoskeletal changes, are not affected by the absence of N-WASP. The origin of epidermal ulcers in N-WASP EKO mice therefore remains unclear. It is known, however, that alopecia and ulcers may result from defects in desmosomes (48). Importantly, establishment of AJs, a process driven by filopodia extension, precedes and possibly assists formation of desmosomes (14). It is therefore possible that deletion of N-WASP, which has been shown to regulate filopodia extension in some experimental systems (32, 49), negatively affects formation of AJ and desmosomes and potentially leads to epidermal ulcers.

Progressive HF cycling defect in N-WASP–deficient epidermis. As early as 8 weeks of age, N-WASP deficiency in unmanipulated skin is associated with a marked increase in the number of follicles entering the first postnatal anagen phase after the complete excision of N-WASP. The large increase in anagen-phase follicles at this time point may result from either a delay in EKO mice progressing from the first postnatal anagen phase or an accelerated onset into the second postnatal anagen phase. By 10 weeks of age, EKO mice exhibit a rapid decline of anagen-phase follicles, which constitute less than 5% of HFs at 10 and 13 weeks of age. This is in contrast to WT mice, which exhibit a progressive increase in the number of anagen-phase HFs between 7 and 13 week of age. In addition, in synchronized hair, there is a HF cycling block that progresses over time from a partial block between 8 to 13 weeks to a complete block by the 20th week of mouse life. This gradual phenotype development may result from the effect of N-WASP ablation on the proliferation and long-term maintenance of HF stem cells. Consistent with this, we observed a dramatically expanded population of proliferating, BrdU-incorporating $CD34^+/\alpha6^+$ skin progenitor cells in N-WASP EKO mice at 8 weeks of age. However, this population is severely depleted by 28 weeks of age, which we hypothesize occurs as a result of continued high levels of proliferation. Interestingly, skin from EKO mice also exhibited an expanded and abnormally persisting population of $CD34^{lo/-}/\alpha6^{lo}$ cells corresponding to the ORS. The increased proliferation and progressive decrease in $CD34^+/\alpha6^+$ cells, along with the expansion and persistence of the ORS population, suggest that N-WASP deficiency aberrantly regulates stem cell homeostasis and may result in the inability to maintain critical skin progenitors in a quiescent state necessary for the long-term maintenance of these progenitors (50).

N-WASP regulates Wnt signaling and β-catenin–dependent transcription. The most striking finding in this study is that N-WASP is essential for HF cycling and its absence leads to alopecia. Wnt signaling and downstream transcriptional events have been demonstrated to be critical for HF development and cycling (21, 23). A decrease in Wnt-responsive reporter activity, dramatic decreases in levels of GSK-3β phosphorylated on serine 9, along with loss of nuclear β-catenin in follicular keratinocytes and decreased Lef1/Tcf-dependent TopGAL reporter activity in vivo in the absence of N-WASP strongly suggest a link between N-WASP and the Wnt signaling pathway. N-WASP or N-WASP–dependent effector function (actin polymerization through Arp2/3) has yet to be linked to any known members of the Wnt pathway, and the specific binding partner(s) altered by N-WASP deficiency in this context remains unknown. The N-WASP interactor Cdc42 has been directly linked to β-catenin stability and has been shown to play a critical role in hair progenitor cell differentiation (8, 28). Similar to our findings in N-WASP–deficient skin, GSK-3β phosphorylation and nuclear translocation of β-catenin are impaired in epidermis lacking Cdc42 (8). However, due to abnormal differentiation of follicular progenitor cells to epidermal lineages, HFs in animals with β-catenin– and Cdc42-deficient skin are replaced with epidermal cysts (8, 21). Of note, these structures were not detected in N-WASP EKO animals. Such differences may result from the relative delay in the hair cycle block in N-WASP–deficient epidermis when compared with β-catenin– or Cdc42-deficient epidermis (8, 21). Analysis of older N-WASP EKO mice has been problematic, since these animals seldom survive past the age of 20 weeks. Alternatively, N-WASP–deficient HF stem cells may be phenotypically distinct from Cdc42-deficient HF stem cells. Indeed, N-WASP–deficient HF stem cells exhibit excessive proliferation and premature depletion, whereas Cdc42-deficient progenitors show abnormal differentiation with aberrant cell fate decisions (8).

Cdc42 directly binds to and modulates the activity of N-WASP (29), raising the possibility that N-WASP deficiency can alter Cdc42-dependent signals to the Wnt pathway and downstream transcriptional events leading to differentiation of progenitor cells into HFs. Indeed, the Wnt/β-catenin signaling pathway is critical for the temporal regulation of HF cycling and for controlling the proliferation and differentiation of HF stem cells. Along the hair shaft, the highest level of Wnt signaling is found in the terminally differentiating cortical cells, and constitutive expression of a stabilized form of β-catenin results in de novo HF formation and pilomatricomas (20). On the opposite end of the spectrum, ablation of β-catenin in the skin results in the loss of HFs (21). Low levels of nuclear β-catenin may be required to maintain bulge stem cells in a quiescent state, and Wnt signaling is largely absent from the bulge. HF bulge stems cells nonetheless express a number of Wnt receptors, Wnt signaling transcription factors, as well as increased levels of Wnt inhibitors (51), which suggests that their ability to receive and transmit Wnt signals is crucial for the proper response to signals specifying self-renewal and differentiation. We have observed, in the absence of N-WASP, defects in the ability to properly integrate Wnt signals, abnormal telogen-to-anagen transition, and a depletion of HF bulge stem cells over time. Together these data suggest a defect in the ability of cells in the hair germ, or that have recently migrated from the bulge, to properly form the hair shaft in response to Wnt signals. This may be due to an intrinsic defect in the ability of these cells to integrate incoming Wnt signals from the underlying dermal papilla and follicular environment in the absence of N-WASP.

Because N-WASP also plays an important role in cell migration, further work is required to determine whether defective migration of N-WASP–deficient hair germ and/or bulge stem cells prevents these cells from establishing the close contacts between the bulge, hair germ, and dermal papilla necessary for signaling the start of a new anagen phase. Perturbations in the ability of hair germ and ORS keratinocytes to receive and transmit Wnt signals may render them unable to feedback appropriate "stop" signals to proliferating HF progenitors, leading to their progressive depletion and eventual exhaustion and the striking phenotype of complete alopecia. Finally, future studies will be needed to determine the specific mechanism by which N-WASP regulates Wnt signaling and the relative importance of the Wnt signaling abnormalities in contributing to the profound HF defects in N-WASP EKO mice.

Methods

Generation of mutant mice, hair depilation, and preparation of epidermal tissue lysates. Mice bearing a conditional *N-Wasp* KO allele (*N-Wasp*^{L2L}) (33) were crossed with *keratin 5-CrePR1* (*K5-Cre*) transgenic mice (35) (a gift from D. Roop, University of Colorado, Aurora, Colorado, USA) to generate

N-Wasp$^{L2L/L2L}$; K5-Cre mice. Littermate *N-Wasp$^{L2L/+}$; K5-Cre* mice were used as controls in each experiment. To generate WT/TopGal and EKO/TopGAL mice, WT and EKO mice were bred with TopGAL reporter mice (Jackson Laboratories) to generate WT and N-WASP–deficient offspring harboring the *LacZ* gene. Mice were kept in a specific pathogen–free barrier facility at the Massachusetts General Hospital in accordance with the guidelines of the Subcommittee on Research Animal Care of Massachusetts General Hospital. Hair plucking was performed as previously described (52). Briefly, the backs of mice with hair in telogen phase were painted with wax, and embedded hair was gently depilated. Skin samples were collected at various time points, stretched, fixed with formalin, and embedded in paraffin. Specifically, skin samples were harvested 3 and 6 days after depilation to observe follicles in anagen II and IV, respectively. Epidermal keratinocytes were isolated from back or ear of adult mice as previously described (53). Briefly, skin was incubated afloat on a surface of 0.25% trypsin solution (CELLGRO) overnight at 4°C. The epidermis was separated from the dermis, chopped, and incubated in 0.25% trypsin for 10 minutes at 37°C with gentle agitation. Released keratinocytes were strained, pelleted down by centrifugation, and resuspended in Laemmli buffer.

Antibodies. Rabbit polyclonal antibody against N-WASP was generously provided by T. Takenawa (Tokyo University, Tokyo, Japan). Anti–keratin 1, involucrin, filaggrin, and loricrin antibodies were purchased from Babco. Rabbit anti–Ki-67 antibodies were purchased from Novocastra Laboratories. Anti–GSK-3β, phospho–GSK-3β (serine 9) antibodies were purchased from Cell Signaling Technology. Anti–E-cadherin and anti-Cdc42 antibodies were purchased from Transduction Laboratories. Alexa Fluor 647–conjugated anti-CD34 was purchased from BD Biosciences, and PE-conjugated anti-CD49f (α6 integrin) was purchased from eBioscience. Anti-BrdU antibodies were purchased from Becton Dickinson. Monoclonal anti–α-tubulin and anti–β-catenin antibodies were purchased from Sigma-Aldrich.

Histology and immunostaining. Paraffin sections of skin tissue were processed for H&E staining. Paraffin and cryostat sections were immunostained with the antibodies against BrdU, Ki-67, and differentiation markers as previously described (54, 55). β-Catenin immunostaining protocol was provided by C. Brakebusch (Copenhagen University, Copenhagen, Denmark). Cultured primary keratinocytes were fixed with 3.7% paraformaldehyde for 10 minutes, permeabilized with 0.2% Triton X-100 for 5 minutes, and stained with either phalloidin (Molecular Probes) or primary antibodies for 1 hour, followed by 1 hour of incubation with secondary antibodies (Jackson Immunoresearch Laboratories Inc.). Fluorescein Mouse-On-Mouse secondary antibody kit (Vector) was used to detect mouse monoclonal antibodies on mouse tissue sections.

X-gal staining. Frozen sections (5 μm) of non-depilated dorsal back skin from WT/TopGAL and EKO/TopGAL mice were fixed in LacZ fixation buffer containing 0.2% glutaraldehyde, then washed with LacZ wash buffer (2 mM MgCl, 0.01% deoxycholate, 0.2% NP-40). Slides were incubated with 5-bromo-4-chloro-3-indolyl-β-D-galactopyranoside (X-gal; Fisher Scientific) for 12 hours in the dark at 37°C. Slides were then washed 3 times in PBS, followed by a water rinse and mounted with glycerol and examined by light microscopy. Coverslips were then removed with water, and slides were counterstained with either nuclear Fast Red or DAPI for 2 minutes. Key HF structures (bulge, hair germ, and dermal papilla) as determined by counterstaining (data not shown) are noted in Figure 6E (inset).

Microscopy. Histological and immunofluorescence analysis was performed with an Olympus AX-70 upright fluorescence microscope.

Cell culture, plasmid transfections, and luciferase assay. Primary keratinocytes were isolated from the skin of 3-day-old mice as previously described (53). Cells were plated on collagen I–coated plastic, with culture medium changed daily. Mouse embryonic fibroblasts were cultured in DMEM supplemented with 10% bovine calf serum (GIBCO). For luciferase reporter assay, fibroblasts were seeded on 24-well plates (Corning) and transfected using Lipofectamine 2000 transfection reagent (Invitrogen) with TopFLASH or FopFLASH expression plasmids (provided by B. Vogelstein, Johns Hopkins University, Baltimore, Maryland, USA). Each well was cotransfected with Renilla luciferase expression vector (pRL-CMV; Promega) for normalization. Eighteen hours after transfection, cells were incubated with conditioned medium from Wnt-3a– and Wnt-5a–expressing cells (as a negative control; CRL-2647 and CRL-2814; ATCC) for 24 hours. Cells were lysed and firefly and Renilla luciferase activities were measured using the Dual Luciferase Reporter kit (Promega). Firefly luciferase signal was normalized to Renilla luciferase activity. Each point was performed in triplicate. Experiments involving N-WASP–deficient fibroblasts used a previously generated KO cell line (32). For N-WASP overexpression studies, WT fibroblasts were transduced with N-WASP–expressing retrovirus, and stable overexpression of protein was confirmed after multiple passages by Western blot analyses.

FACS analysis. Fat and subcutaneous tissues were removed from the back skin of 10 adult WT and 11 EKO mice at 8, 16, or 28 weeks of age. After floating overnight on 0.25% trypsin at 4°C, the epidermis was separated from the dermis with a forceps, finely minced, and passed through a 100-μm filter followed by a 70-μm filter to remove cornified sheets. The resulting single-cell suspension was then washed and resuspended in PBS with 1% FCS and incubated with 0.5 mg/ml Alexa Fluor 647–conjugated rat anti-mouse CD34 (BD Biosciences) and 0.5 mg/ml phycoerythrin-conjugated (PE-conjugated) anti-human/mouse CD49f (α6 integrin; eBioscience) for 30 minutes on ice. After washing twice in PBS with 1% FCS, cells were subjected to FACS analysis. BrdU detection was performed with a BD Biosciences — Pharmingen FITC BrdU Flow Kit.

Keratinocyte proliferation analysis. Adherent cultured keratinocytes were exposed to BrdU (Amersham Biosciences) for 30 minutes at a concentration recommended by the manufacturer. For analysis by flow cytometry, cells were detached by trypsinization, stained, and analyzed as described by Becton-Dickinson protocol. For proliferation analysis in vivo, mice were injected intraperitoneally with 50 μg/g body weight BrdU (10 mg/ml in PBS) 2 hours prior to sacrifice. To detect proliferating keratinocytes, paraffin skin sections were made and processed for immunohistochemistry as previously described (55).

Epidermal wound healing assay. Full-thickness 6-mm-diameter circular wounds were made on back skin of 8-week-old mice matched by sex under avertin anesthesia. Wounds were left undressed, and animals were individually housed. After 1, 3, and 4 days, the animals were sacrificed, and wound tissue was harvested and examined histologically.

Statistics. Data are presented as mean ± SEM unless otherwise specified. Groups were compared by unpaired 2-tailed Student's *t* test. A *P* value less than 0.05 was considered significant.

Acknowledgments

We thank Alexander van Oudenaarden and members of the Snapper laboratory for critical reading of this manuscript. This work was funded in part by NIH grant 5P01 HL59561 to S.B. Snapper.

Received for publication September 8, 2009, and accepted in revised form November 19, 2009.

Address correspondence to: Scott B. Snapper, Massachusetts General Hospital, Gastrointestinal Unit, 55 Fruit St., Jackson 825c, Boston, Massachusetts 02114, USA. Phone: (617) 724-8809; Fax: (617) 643-0195; E-mail: ssnapper@hms.harvard.edu.

1. Cotsarelis G, Sun TT, Lavker RM. Label-retaining cells reside in the bulge area of pilosebaceous unit: implications for follicular stem cells, hair cycle, and skin carcinogenesis. *Cell*. 1990;61(7):1329–1337.
2. Donaldson DJ, Mahan JT. Keratinocyte migration and the extracellular matrix. *J Invest Dermatol*. 1988;90(5):623–628.
3. Fuchs E, Merrill BJ, Jamora C, DasGupta R. At the roots of a never-ending cycle. *Dev Cell*. 2001;1(1):13–25.
4. Carreira S, et al. Mitf regulation of Dia1 controls melanoma proliferation and invasiveness. *Genes Dev*. 2006;20(24):3426–3439.
5. Waschke J, et al. Inhibition of Rho A activity causes pemphigus skin blistering. *J Cell Biol*. 2006;175(5):721–727.
6. Benitah SA, Frye M, Glogauer M, Watt FM. Stem cell depletion through epidermal deletion of Rac1. *Science*. 2005;309(5736):933–935.
7. Chrostek A, et al. Rac1 is crucial for hair follicle integrity but is not essential for maintenance of the epidermis. *Mol Cell Biol*. 2006;26(18):6957–6970.
8. Wu X, et al. Cdc42 controls progenitor cell differentiation and beta-catenin turnover in skin. *Genes Dev*. 2006;20(5):571–585.
9. Ehrlich JS, Hansen MD, Nelson WJ. Spatio-temporal regulation of Rac1 localization and lamellipodia dynamics during epithelial cell-cell adhesion. *Dev Cell*. 2002;3(2):259–270.
10. Etienne-Manneville S, Hall A. Rho GTPases in cell biology. *Nature*. 2002;420(6916):629–635.
11. Noren NK, Niessen CM, Gumbiner BM, Burridge K. Cadherin engagement regulates Rho family GTPases. *J Biol Chem*. 2001;276(36):33305–33308.
12. Vaezi A, Bauer C, Vasioukhin V, Fuchs E. Actin cable dynamics and Rho/Rock orchestrate a polarized cytoskeletal architecture in the early steps of assembling a stratified epithelium. *Dev Cell*. 2002;3(3):367–381.
13. Vasioukhin V, Fuchs E. Actin dynamics and cell-cell adhesion in epithelia. *Curr Opin Cell Biol*. 2001;13(1):76–84.
14. Vasioukhin V, Bauer C, Yin M, Fuchs E. Directed actin polymerization is the driving force for epithelial cell-cell adhesion. *Cell*. 2000;100(2):209–219.
15. Logan CY, Nusse R. The Wnt signaling pathway in development and disease. *Annu Rev Cell Dev Biol*. 2004;20:781–810.
16. Clevers H. Wnt/beta-catenin signaling in development and disease. *Cell*. 2006;127(3):469–480.
17. Huang H, He X. Wnt/beta-catenin signaling: new (and old) players and new insights. *Curr Opin Cell Biol*. 2008;20(2):119–125.
18. Reya T, Morrison SJ, Clarke MF, Weissman IL. Stem cells, cancer, and cancer stem cells. *Nature*. 2001;414(6859):105–111.
19. Alonso L, Fuchs E. Stem cells in the skin: waste not, Wnt not. *Genes Dev*. 2003;17(10):1189–1200.
20. Gat U, DasGupta R, Degenstein L, Fuchs E. De novo hair follicle morphogenesis and hair tumors in mice expressing a truncated beta-catenin in skin. *Cell*. 1998;95(5):605–614.
21. Huelsken J, Vogel R, Erdmann B, Cotsarelis G, Birchmeier W. beta-Catenin controls hair follicle morphogenesis and stem cell differentiation in the skin. *Cell*. 2001;105(4):533–545.
22. van Genderen C, et al. Development of several organs that require inductive epithelial-mesenchymal interactions is impaired in LEF-1-deficient mice. *Genes Dev*. 1994;8(22):2691–2703.
23. Andl T, Reddy ST, Gaddapara T, Millar SE. WNT signals are required for the initiation of hair follicle development. *Dev Cell*. 2002;2(5):643–653.
24. Ito M, Yang Z, Andl T, Cui C, Kim N, Millar SE, Cotsarelis G. Wnt-dependent de novo hair follicle regeneration in adult mouse skin after wounding. *Nature*. 2007;447(7142):316–320.
25. Merrill BJ, Gat U, DasGupta R, Fuchs E. Tcf3 and Lef1 regulate lineage differentiation of multipotent stem cells in skin. *Genes Devel*. 2001;15(13):1688–1705.
26. DasGupta R, Fuchs E. Multiple roles for activated LEF/TCF transcription complexes during hair follicle development and differentiation. *Development*. 1999;126(20):4557–4568.
27. Tiede S, Kloepper JE, Bodo E, Tiwari S, Kruse C, Paus R. Hair follicle stem cells: walking the maze. *Eur J Cell Biol*. 2007;86(7):355–376.
28. Etienne-Manneville S, Hall A. Cdc42 regulates GSK-3beta and adenomatous polyposis coli to control cell polarity. *Nature*. 2003;421(6924):753–756.
29. Miki H, Takenawa T. Regulation of actin dynamics by WASP family proteins. *J Biochem*. 2003; 134(3):309–313.
30. Ridley AJ. Rho GTPases and actin dynamics in membrane protrusions and vesicle trafficking. *Trends Cell Biol*. 2006;16(10):522–529.
31. Lommel S, Benesch S, Rottner K, Franz T, Wehland J, Kuhn R. Actin pedestal formation by enteropathogenic Escherichia coli and intracellular motility of Shigella flexneri are abolished in N-WASP-defective cells. *EMBO Rep*. 2001;2(9):850–857.
32. Snapper SB, et al. N-WASP deficiency reveals distinct pathways for cell surface projections and microbial actin-based motility. *Nat Cell Biol*. 2001;3(10):897–904.
33. Cotta-de-Almeida V, et al. Wiskott Aldrich syndrome protein (WASP) and N-WASP are critical for T cell development. *Proc Natl Acad Sci U S A*. 2007;104(39):15424–15429.
34. Nelson WG, Sun TT. The 50- and 58-kd keratin classes as molecular markers for stratified squamous epithelia: cell culture studies. *J Cell Biol*. 1983;97(1):244–251.
35. Zhou Z, Wang D, Wang XJ, Roop DR. In utero activation of K5.CrePR1 induces gene deletion. *Genesis*. 2002;32(2):191–192.
36. Minamino T, Gaussin V, DeMayo FJ, Schneider MD. Inducible gene targeting in postnatal myocardium by cardiac-specific expression of a hormone-activated Cre fusion protein. *Circ Res*. 2001;88(6):587–592.
37. Watt FM. Role of integrins in regulating epidermal adhesion, growth and differentiation. *EMBO J*. 2002;21(15):3919–3926.
38. Fuchs E. Epidermal differentiation: the bare essentials. *J Cell Biol*. 1990;111(6 Pt 2):2807–2814.
39. Dotto GP. Signal transduction pathways controlling the switch between keratinocyte growth and differentiation. *Crit Rev Oral Biol Med*. 1999;10(4):442–457.
40. Muller-Rover S, et al. A comprehensive guide for the accurate classification of murine hair follicles in distinct hair cycle stages. *J Invest Dermatol*. 2001;117(1):3–15.
41. Blanpain C, Lowry WE, Geoghegan A, Polak L, Fuchs E. Self-renewal, multipotency, and the existence of two cell populations within an epithelial stem cell niche. *Cell*. 2004;118(5):635–648.
42. Jaks V, et al. Lgr5 marks cycling, yet long-lived, hair follicle stem cells. *Nat Genet*. 2008;40(11):1291–1299.
43. Blanpain C, Fuchs E. Epidermal stem cells of the skin. *Annu Rev Cell Dev Biol*. 2006;22:339–373.
44. Nowak JA, Fuchs E. Isolation and culture of epithelial stem cells. *Methods Mol Biol*. 2009;482:215–232.
45. Martin TA, Pereira G, Watkins G, Mansel RE, Jiang WG. N-WASP is a putative tumour suppressor in breast cancer cells, in vitro and in vivo, and is associated with clinical outcome in patients with breast cancer. *Clin Exp Metastasis*. 2008;25(2):97–108.
46. Grone A. Keratinocytes and cytokines. *Vet Immunol Immunopathol*. 2002;88(1–2):1–12.
47. Nguyen DD, et al. Lymphocyte-dependent and Th2 cytokine-associated colitis in mice deficient in Wiskott-Aldrich syndrome protein. *Gastroenterology*. 2007;133(4):1188–1197.
48. Bazzi H, Christiano AM. Broken hearts, woolly hair, and tattered skin: when desmosomal adhesion goes awry. *Curr Opin Cell Biol*. 2007;19(5):515–520.
49. Miki H, Sasaki T, Takai Y, Takenawa T. Induction of filopodium formation by a WASP-related actin-depolymerizing protein N-WASP. *Nature*. 1998;391(6662):93–96.
50. Orford KW, Scadden DT. Deconstructing stem cell self-renewal: genetic insights into cell-cycle regulation. *Nat Rev Genet*. 2008;9(2):115–128.
51. Tumbar T, et al. Defining the epithelial stem cell niche in skin. *Science*. 2004;303(5656):359–363.
52. Paus R, Stenn KS, Link RE. Telogen skin contains an inhibitor of hair growth. *Br J Dermatol*. 1990;122(6):777–784.
53. Missero C, Di Cunto F, Kiyokawa H, Koff A, Dotto GP. The absence of p21Cip1/WAF1 alters keratinocyte growth and differentiation and promotes ras-tumor progression. *Genes Dev*. 1996;10(23):3065–3075.
54. Foitzik K, Paus R, Doetschman T, Dotto GP. The TGF-beta2 isoform is both a required and sufficient inducer of murine hair follicle morphogenesis. *Dev Biol*. 1999;212(2):278–289.
55. Mizoguchi E, Mizoguchi A, Bhan AK. Role of cytokines in the early stages of chronic colitis in TCR alpha-mutant mice. *Lab Invest*. 1997; 76(3):385–397.